

A Relation between Tensile and Tear Strength for Design of Architectural Fabrics

STRUCTURAL MEMBRANES 2015

Keith M. MacBain Ph.D., P.E.* , and David M. Campbell P.E.†

* Geiger Gossen Campbell Engineers, P.C.
2 Executive Blvd. Suite 309, Suffern, NY 10901, USA
e-mail: kmm@geigerengineers.com, web page: <http://www.geigerengineers.com>

† Geiger Gossen Campbell Engineers, P.C.
e-mail: dmc@geigerengineers.com, web page: <http://www.geigerengineers.com>

Key words: Fabric strength, tear strength, tear propagation, structural design

Summary. This paper presents a model that relates tensile and tear strengths for architectural fabrics used in tension membrane structures. Extension of the model is also presented as a means to use these two material strengths in establishing an allowable size of defects in a given field of stress.

1. Introduction

Two commonly used methods are available for testing and reporting the strength of architectural fabrics. These are the (strip) tensile and the trapezoidal tear tests. Design of fabric structures is commonly based on the tensile strength of the fabric, typically using a large factor of safety (4 or 5) to account for various uncertainties. It is well regarded however that tensile failure is typically not the mode of failure but rather tear. Currently the designer has limited opportunity to recognize tear strength in the design, despite this being the more common mode of failure.

2. Trapezoid Test

The trapezoid tear test of ASTM D5587 is the basis for discussion however the development herein may be applied to similar tests such as EN 1875-3. A generic figure of the sample is given below, which also establishes a local coordinate axis taken parallel to the slit with the origin at the edge of the slit and positive in the direction of expected tear propagation.

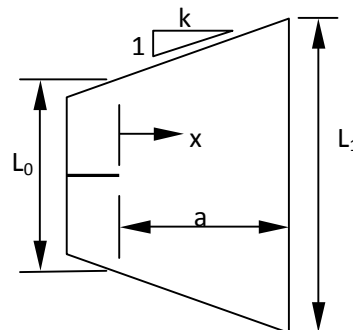


Figure 1: Generic Test Specimen

Because the non-parallel sides of the specimen are placed in parallel grips, there is an initial gap (slackness) that varies over the transverse coordinate x . Denoting the gap as $g(x)$, and considering there to be initially no slackness at $x = 0$, the initial gauge length of the sample is given as

$$\begin{aligned} L(x) &= L_0 + g(x) \\ &= L_0 + \frac{L_1 - L_0}{a}x \end{aligned} \quad (1)$$

As the test proceeds, the elongation of the sample in the machine direction is taken to vary linearly over the transverse coordinate x , with a step function to account for the initial slackness at $x > 0$. This elongation is shown below at some time before tear propagation along with the total machine displacement d_M relative to the point when there is no slackness at the initial edge of the slit.

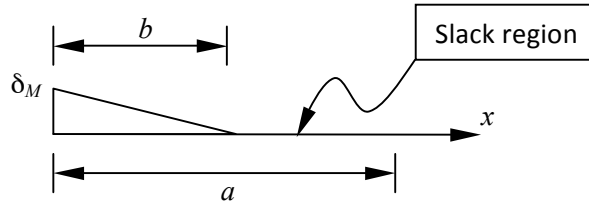


Figure 2: Elongation versus Transverse Coordinate

The strain in the sample is then expressed simply as the change in length divided by the initial gauge length. Because the gauge length also varies with x , this results in the nonlinear relation given below, where $H(x)$ is the Heaviside step function.

$$\varepsilon(x) = H(b-x)\delta_M \frac{k}{b} \left(\frac{b-x}{kL_0 + 2x} \right) \quad (2)$$

In the above, the change in initial gauge length is represented by the term with x in the denominator. If $2x$ is small compared to kL_0 , this term may be ignored and the above reduces to a linear relation equivalent to that of a constant gauge length L_0 over the entire transverse length. This simplified strain distribution follows the same form as the elongation shown above and will be used for further development.

For ease of development, a linear stress-strain relation is assumed. It will be seen later however, that this is linear assumption is not essential for application of the model developed here. For clarity, throughout this paper the term stress is not used in the classical engineering sense of force divided by area but rather the commonly adopted usage in the fabric industry of force divided by length (i.e., the thickness is disregarded). Using the subscript 0 for terms evaluated at $x = 0$ and similarly the subscript b for terms evaluated at $x = b$ gives the following relations.

$$\begin{aligned}\delta_M &= \varepsilon_0 L_0 \\ g_b &= \frac{b}{a}(L_1 - L_0) = \delta_M \quad \Rightarrow \quad b = \frac{a\varepsilon_0 L_0}{L_1 - L_0} = \frac{k}{2}\varepsilon_0 L_0\end{aligned}\quad (3)$$

The total force F in this idealized stress distribution is simply the area under the triangle.

$$F = \frac{\mu}{2}\sigma_0 b; \quad \mu = 1 \quad (4)$$

The constant m is introduced at this point only for the purpose of later discussion. It will be termed here as the ductility parameter because it determines the area under the stress-strain curve based on the shape, the extreme stress, and the distance. Introducing the material stiffness E (units of force per length) and assembling these relations allows the above to be cast in in the following form.

$$F = \mu \frac{k}{4} \frac{\sigma_0^2}{E} L_0 \quad (5)$$

The above equation will be referred to later as the tensile-tear relation, because it relates the peak tensile stress to the total force in a trapezoidal tear test. It is noted that this is not an empirical relation but rather one derived from basic engineering mechanics and the linear assumptions given herein. Unless noted otherwise, a unit ductility parameter ($m = 1$) will be used throughout this paper. Similarly, the parameters derived from the ASTM D4851 test specimen of $k = 2$ and $L_0 = 40$ mm (1.6 in) will be used.

3. Nonlinear Considerations

The development of the above included some linear approximations. It is argued here that these do not need to be adhered to strictly in order to apply the tensile-tear relation.

The assumption of a constant gauge length that resulted in a linear strain distribution is considered first. The correct relation for the total force without this assumption (but still maintaining the linear stress-strain assumption) is expressed below.

$$F = \int_0^b \sigma(x) dx = \int_0^b E\varepsilon(x) dx \quad (6)$$

This function is evaluated numerically using the nonlinear strain equation presented earlier and compared in the figure below with the force computed by the linear strain assumption.

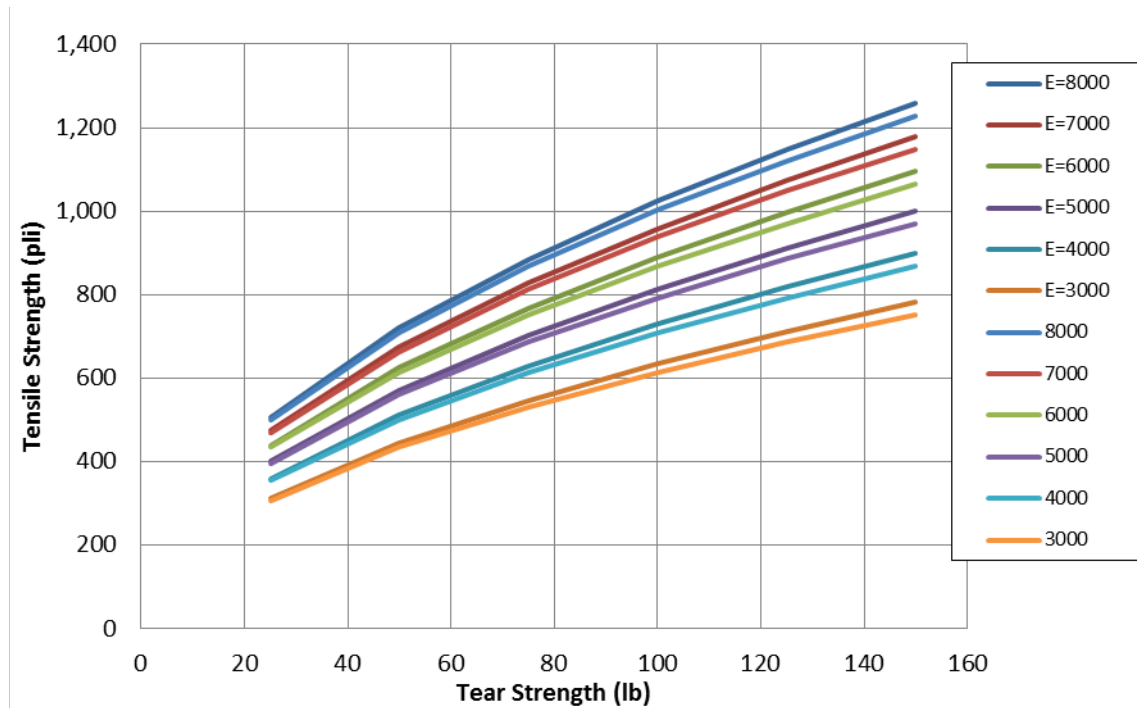


Figure 3: Tensile Strength v. Tear Strength

Parameters used in the figure above are $m = 1$, $k = 2$, and $L_0 = 1.6''$. It is noted that the lines from the two methods are clearly divergent (i.e., the difference increases with force) however in the selected range, the difference appears to be within the variability associated with test data. For clarity, this is the only consideration given in this paper to the full nonlinear strain relation and all remaining work is based on the tensile-tear relation developed with the linear strain assumption.

Fabric generally exhibits a nonlinear stress-strain relation, which is thought to be well addressed in this model by the ductility parameter m . This use bears strong analogy to the model of the Whitmore stress block commonly used for concrete. From a design point of view, the actual stress distribution is typically of less interest than the load-carrying capacity. It is thought that this parameter would be material-specific and in this regard, the specific nature of the ductility (e.g, material yielding, yarn mobility, weave type, coating stiffness) is of less concern than simply its existence or lack thereof. For example, the stress distribution associated with peak tear strength might have the form given below and a m value determined from the area under the curve.

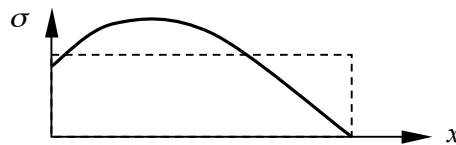


Figure 4: Conceptual use of m for Nonlinear Material

The determination of this parameter is beyond the scope of this work however it is thought that material test data and the tensile-tear model could be readily used for this purpose. Specifically, given the values k and L_0 for a particular test method (e.g., ASTM D4851), the manufacturer's reported values for tear strength and tensile strength could be used to solve for m in the tensile-tear relation. Numerical evaluation might be used as well provided that the nonlinear material parameters are reasonably quantified.

4. Product Comparison

The tensile-tear relation is compared with manufacturer's test data for PTFE woven fabric from St. Gobain. In this comparison, the same $L_0 = 1.6''$ derived from ASTM D4851 is used along with the ductility parameter $m = 1$.

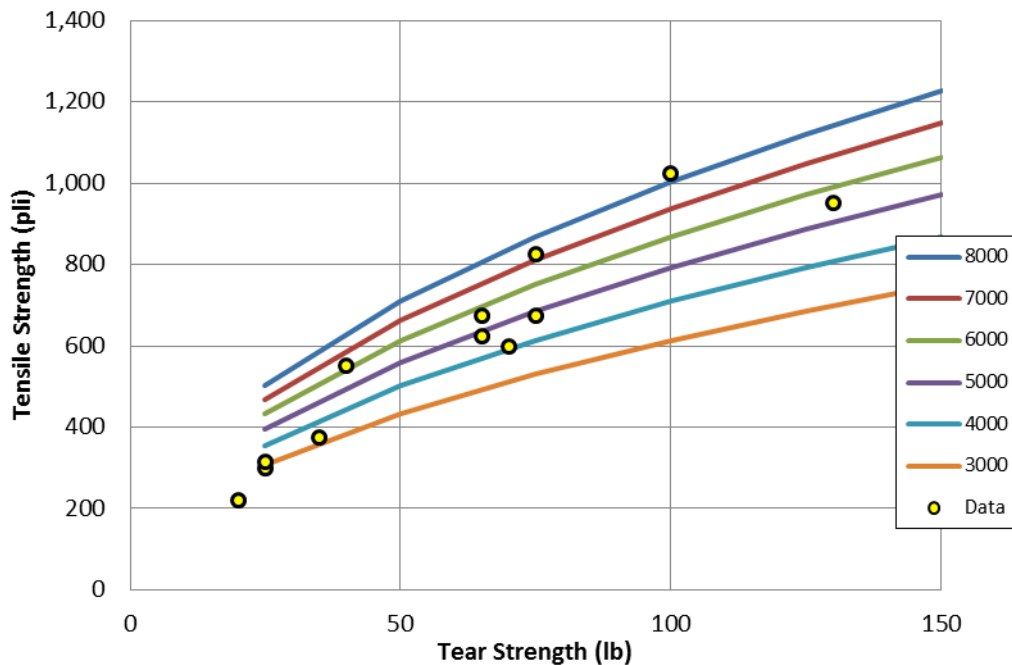


Figure 5: Tensile-Tear Relation vs. Product Data

There is generally little material ductility associated with fiberglass therefore the selected ductility parameter $m = 1$ appears appropriate. As noted earlier, different values of m may be appropriate for different materials and is thought to give an indication of the overall ductility of the fabric as a system, irrespective of the exact nature of the ductility (e.g., material yielding, yarn mobility, ...).

5. Application

The tensile-tear relation can be applied in evaluating the potential for tear propagation in a constant stress field. In this development, it is assumed that the stress is uniform in a given direction however

not necessarily equal in the two material directions. The development here is first given for a uniaxial stress field as follows and then modified as will be seen later.

The concept in applying this model is that the net force in the cut must be redistributed to nearby regions. The ability for the nearby regions to realize this force is assumed to be related to the trapezoid tear strength according to the tensile-tear model. Again returning to a linear model for ease of development, the stress distribution normal to the axis of a cut with a length c is shown below.

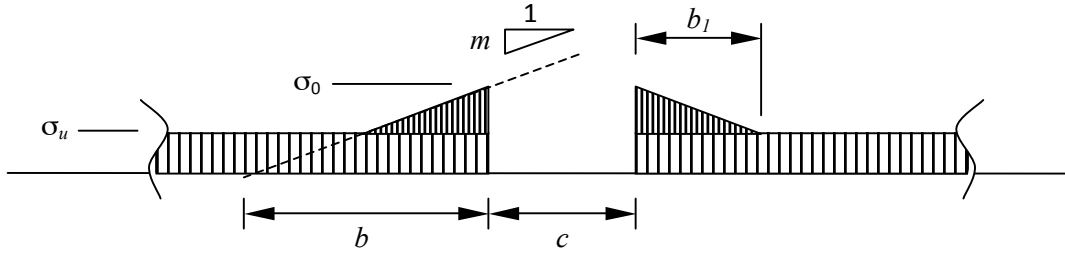


Figure 6: Assumed Stress Distribution in Vicinity of Cut

The term s_u is the uniform stress level in an infinite field. The local increase to level s_0 in the vicinity of the cut is necessary to maintain equilibrium. The slope of the linearly varying portion is then estimated from the tensile-tear model by the relation below.

$$m = \frac{\sigma_0}{b} = \frac{\mu\sigma_0^2}{F} \quad (7)$$

Based on force equilibrium, the following is obtained.

$$c\sigma_u = (\sigma_0 - \sigma_u)b_1 \quad (8)$$

Using this relation and the slope presented above, a quadratic equation in s_u appears which has the roots given below.

$$\sigma_u = \frac{1}{2} \left\{ (2\sigma_0 + cm) \pm \sqrt{(2\sigma_0 + cm)^2 - 4\sigma_0^2} \right\}$$

The above form makes it clear that the smaller root is of interest however it is more readily applied when the slope m is removed from the equation. Selecting the smaller root and making this substitution gives the form below.

$$\sigma_u = \frac{1}{2} \left\{ 2\sigma_0 + \frac{cE}{\mu k L_0} - \sqrt{\frac{cE}{\mu k L_0} \left(4\sigma_0 + \frac{cE}{\mu k L_0} \right)} \right\} \quad (10)$$

The above form is appealing because it expresses the peak magnitude of an otherwise uniform stress field (s_u) in the presence of a cut with a length c in terms of only the material properties (s_0, E, m) and the geometry of the trapezoidal tear test specimen (k, L_0). It is noted that as c approaches zero, the full peak tensile strength is predicted. Further, it is noted that although the trapezoid tear strength does not explicitly appear in the equation, it was used in the development and appears implicitly through the geometry of the test sample and the ductility parameter.

6. Comparison with Other Models

The model above is compared with two other proposed models. These are both empirical models and although they employ the results of the trapezoid tear test, they do not explicitly consider the specimen geometry.

The first is an early development used in-house by Geiger Gossen Campbell Engineers which expresses the maximum stress S_{max} in terms of the strip tensile strength S_{st} , the tear strength R_{ult} , and the maximum cut length L_{max} by the two equations given below and termed the GGC model.

$$\begin{aligned} S_{max} &\leq L_t \phi_T S_{st} \\ S_{max} &\leq L_t \phi_F \left(\frac{2R_{ult}}{L_{max}} \right) \end{aligned} \quad (11)$$

The term L_t is a life-cycle factor (specified by the manufacturer) and f is a resistance factor with regard to tension failure (f_T) or tear failure (f_F). The values for these parameters are not of interest in this paper however for reference $L_t = 0.75$, $f_T = 0.33$, and $f_F = 0.625$ are not uncommon depending on the material. Clearly the first equation is related to ordinary tensile strength evaluation and the second considers tear strength. Only the second is of interest in this paper.

The second model considered here is that proposed by Rendely¹. Using the notation above the relation presented is reproduced below.

$$L_{max} = \left(C_1 \left(\frac{R_{ult}}{S_{st}} \right)^{C_2} \left(\frac{S_{st}}{S_{max}} \right)^{C_3} \right)^{C_4} \quad (12)$$

It is first noted that this model contains four constants but only three are unique (i.e., the above may be reduced to a form with only three constants). It may be envisioned however that four are more convenient as there is discussion of specific phenomena that might be associated with each. In light of this, it is also noted that for the model to be dimensionally correct, the constraint arises that the product $C_2 C_4$ must be equal to one which, although not mentioned, could also be the intent of using four constants. It is inferred that the above form is to be used in conjunction with an additional evaluation of ordinary tensile strength similar to the first of two equations presented above in the GGC model. Constants presented by Rendely¹ for initial evaluation are $C_1 = 1$, $C_2 = 0.5$, $C_3 = 2$, and $C_4 = 0.5$ and this particular set does not result in a dimensionally correct model. These three models are

compared in the figure below for an arbitrarily chosen example of $S_{st} = 92 \text{ kN/m}$ (525 pli) and $R_{ult} = 311 \text{ N}$ (70 lb) only to examine the trends.

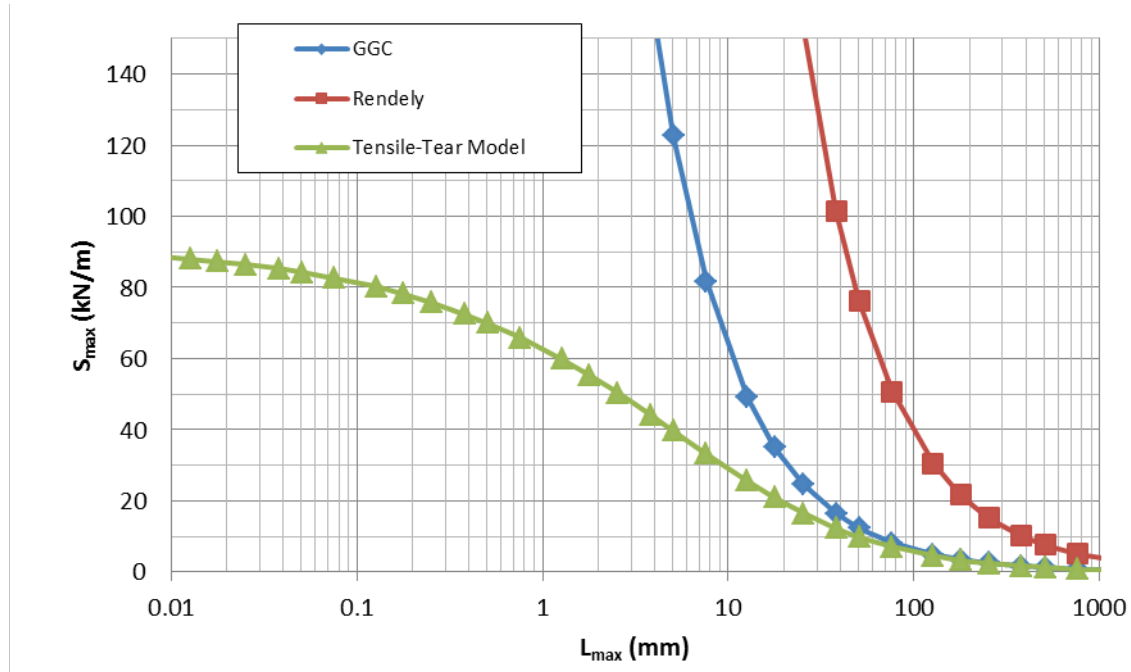


Figure 7: Comparison of Tensile-Tear Models

As noted earlier, it is clear to see from the above that as the cut length approaches zero in the tensile-tear model, the predicted strength approaches the tensile strength. This is in contrast to the other two models compared here, in which the tensile strength approaches infinity, of course requiring them to be used in conjunction with the ordinary tensile strength evaluation.

Because the comparison models approach infinity as the cut length becomes smaller, they are more useful for quantifying the effect larger cuts than small manufacturing defects. In this example, a defect smaller than 40 mm for the Rendely¹ model (7 mm for the GGC model) predicts a tensile strength greater than the strip tensile strength, which renders these models useless for defects below this range. It is thought that this makes the present model particularly appealing as it is well suited to accounting for some small quantifiable random defect, particularly if such defect is inherent in manufacturing.

The two relations presented here for comparison appear to exhibit the same trend throughout, differing only in the selected constants.

7. Bi-Axial Stress Field

The above is based on uniaxial stress field. To extend the application to a biaxial field the following concept is presented. A transverse stress s_x is expected to cause a restoring stress s_r in the vicinity of a

cut. This is conceptually similar to a uniform lateral force on a cable where s_r is related to the transverse force and s_x is related to the tension.

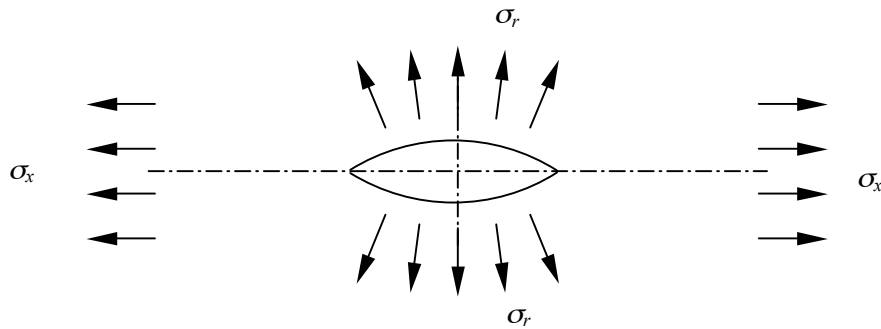


Figure 8: Assumed Stress Components in Vicinity of Cut

Not shown in the figure above is the overall stress in the direction transverse to the cut, which serves to open the cut. The restoring stress will serve to decrease the peak stress s_0 at the face of the cut shown in Figure xx. For clarity, this is considered here to be a simple model of a more complex phenomenon and unrelated to Poisson's ratio. Given this notion, it only remains to quantify this restoring stress and the model presented below.

$$\sigma_r = \sigma_y \left(1 - e^{-C_1 \left(\frac{\sigma_x}{\sigma_y} \right)^{C_2}} \right) \quad (13)$$

Clearly this simplification ignores many aspects, including shear transfer within the fabric some distance away from the cut. The above form is presented here primarily for consideration by future researchers. It is based on the notion that the restoring stress is zero in the absence of a transverse stress and approaches s_u as the transverse stress approaches infinity.

Determination of the appropriate constants for different materials is outside the scope of this work however a computer model was constructed and small amount of numerical evaluation is used to verify the behavior and give initial values. As such, parameters of this model are not important however they are given here for reference. Selected values are moduli of $E_x = E_y = 875 \text{ kN/m}$ (5000 pli), reference load of $s_y = 23 \text{ kN/m}$ (133 pli), grid spacing of 19 mm (0.75 in) and a cut length of 76 mm (3 in). The figure below shows the model in a deformed configuration (i.e., with the cut open).

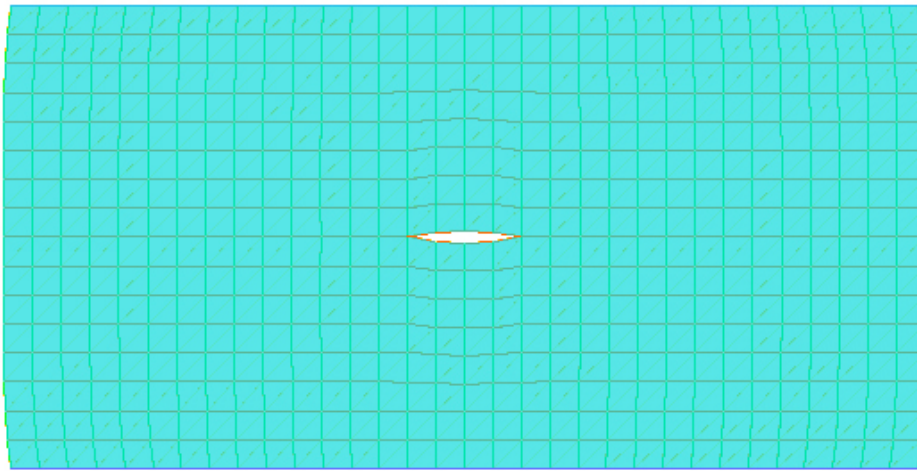


Figure 9: Numerical Model with Cut

The normal stress s_y in the vicinity of the cut is averaged for different values of the transverse stress s_x and these are termed s_r for the purpose of developing this model. Computed values are divided by the nominal normal stress and shown below together with the model presented above using the constants $C_1 = 0.05$ and $C_2 = 0.5$.

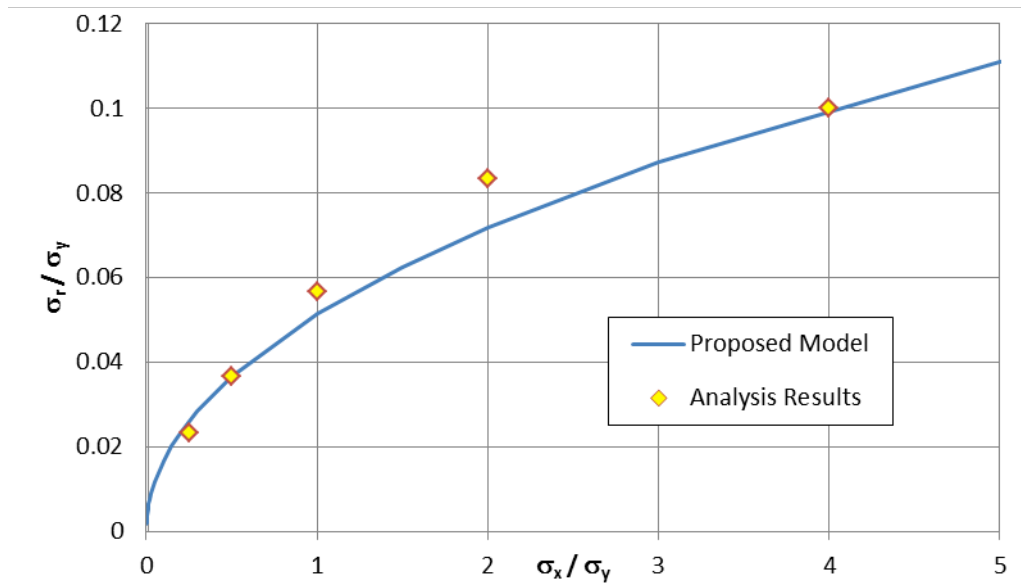


Figure 10: Computer Results vs. Proposed Model

As noted above, further development of this model is outside the scope of this work. However, it is thought that this is a reasonable approach to account for a more complex phenomena and warrants further consideration. The main intent of this model is to provide some means of accounting for a

biaxial stress field. In this regard, the tensile-tear relation given above is augmented to include this reduction from s_r with the following replacement.

$$\sigma_0 \leftarrow \sigma_0 + \sigma_r \quad (14)$$

This gives that the peak tensile stress s_0 accounting for a given imperfection in an otherwise uniform stress field is increased according to the presence of the restoring stress s_r . It is recommended that further development of this model consider also the length of cut in determining s_r so that it does not artificially increase s_0 .

8. Conclusions

A dimensionally correct model was presented that relates trapezoid tear strength to tensile strength. Good correlation with manufacturer's data is seen. Further study is needed to examine a variety of different materials and products.

This model can be employed as a means to use these two material strengths in establishing an allowable size of defects in a given field of stress. Comparison is made with results from available test data on the strength of imperfect specimens.

An approach to accounting for the effects of biaxial membrane stresses on the tensile-tear strength relation is suggested but requires further development.

REFERENCES

- [1] W. Rendely, Structural Fabric Tear Propagation, *Proceedings of the 2009 Structures Congress*, 2009, ASCE, Reston, VA, 978-0-78444-1031-8